Desalination and Water Treatment
www.deswater.com

doi: 10.5004/dwt.2017.20135

62 (2017) 403–417
February

Prediction of simultaneous sorption of copper(II), cobalt(II) and zinc(II) contaminants from water systems by a novel multi-functionalized zirconia nanofiber

Mona Modaresi Tehrani[a], Saeed Abbasizadeh[b,*], Amin Alamdari[c], Seyyed Ebrahim Mousavi[b]

[a]*Department of Chemistry, Islamic Azad University, East Tehran Branch, Tehran, Iran, email: m.modarresi.tehrani@gmail.com*
[b]*Department of Chemical Engineering, Tarbiat Modares University, P.O. Box 14115/138, Tehran, Iran, Tel. +98 21 82883337; Fax: +98 21 82883531; emalis: s.abbasizadeh87@gmail.com (S. Abbasizadeh), s.ebrahimmousavi66@gmail.com (S.E. Mousavi)*
[c]*Young Researchers and Elite club, Robatkarim Branch, Islamic Azad University, Robatkarim, Iran, email: aminalamdari82@gmail.com*

Received 2 April 2016; Accepted 6 August 2016

ABSTRACT

In order to evaluate the sorption of copper(II), cobalt(II) and zinc(II) ions from water systems in the batch systems, a novel elecrtospun zirconia modified with thiol and amine groups/Poly vinyl pyrrolidone (APTES/TMPTMS/Zirconia/PVP/P123) was synthesized. The morphology of nanofibers was characterized by FTIR, SEM, BET and BJH analyses. Based on results, the average fiber diameter of APTES/TMPTMS/Zirconia/PVP/P123 adsorbent was found to be 98.9 nm. The adsorption experiments were carried out to investigate the effect of different adsorption parameters such as solution pH, contact time, initial concentration and temperature. The kinetic data of metal ions were well described by the double-exponential model. The maximum sorption capacities of Cu(II), Co(II) and Zn(II) ions were estimated to be 4.146, 3.050 and 2.352 mmol/g, respectively in the single system. In all binary systems, the sorption capacity decreased with increasing the other metal ion concentrations. The combined effect of metal ions onto the nanofiber was found to be antagonistic. The selectivity order of metal ions sorption onto the adsorbent was Cu(II)>Co(II)>Zn(II).

Keywords: Electrospinning; Zirconia; Nanofiber; Sorption; Binary system; Isotherm models

1. Introduction

Water contaminants may include copper, cobalt and zinc metal ions which are poisonous to human, animals and plants. To resolve the problem of heavy metal pollutions, it is necessary to decontaminate the effluents from environment prior to their discharge from mining, metal plating and other industries [1,2]. Several conventional methods have been developed for the removal of heavy metals such as solvent extraction [3], electrocoagulation [4], chemical precipitation and ion exchange [5,6], filtration [7]. Disadvantages of these techniques are high costs for chemicals and materials, complex operational set-up and high energy consumption [8]. Moreover, for diluted solutions, the most of these methods are ineffective for the removal of heavy metal ions from aqueous solutions. In order to reduce the water pollutant, the sorption process is one of the most effective and flexible techniques due to its simplicity, moderate operational conditions and economic feasibility [9–14]. Recently, metal nano-oxides and polymer nanofibers were widely employed for the sorption of heavy metal ions from aqueous solutions due to their large specific surface area, and surface physical and chemical modification properties. For example, zirconia is a useful rare earth metal oxide in the sorption process [15] but, in general, these nano-oxides are in colloidal forms after

* Corresponding author.

sorption process and so they are not suitable for water treatment because the separation of ZrO_2 from aqueous solution is very difficult, specially, when particle size is on a nano-scale. Loading the metal oxide nanoparticles on another support such as polymers is one of the best ways to solve this problem. Besides nanoparticles, zirconia has been successfully fabricated in other forms, such as nanofibers [16]. There are few investigations for the sorption of heavy metal ions by the adsorbents based on zirconia [15]. The nanofiber adsorbents prepared by the electrospinning method have unique properties such as high specific surface area and high porosity with fine pores [16]. Various suitable functional groups such as thio-ether (–S–), thiol (–SH) and amine ($–NH_2$) groups are used to modify the surface of nanofiber adsorbents and these groups can react with the heavy metal ions in the water to form metal ions complex [9,17,18]. Most of the investigation reported in the literature includes single-component sorption of heavy metal ions [16]. It is expected that the sorption capacity can increase with the modification of polymer adsorbents with the multi-functional groups (for example, modification of the adsorbent with the bifunctional groups ($–SH/–NH_2$)). Therefore, the inhibitory effect of the heavy metal ions concentrations on the sorption capacity and study on the simultaneous sorption of heavy metals from binary aqueous systems are very important because the actual wastewater treatment systems often have to deal with a mixture of heavy metals [19]. Competitive sorption of heavy metals by the multi-functionalized Zirconia/ PVP/P123 has never been reported previously.

The present paper aims to (i) characterize the chemical structure and morphology of functionalized Zirconia/PVP/P123 nanofibers by FTIR, SEM, BET and BJH analyses, (ii) investigate the feasibility of using multi-functionalized Zirconia/PVP/P123 nanofiber as an adsorbent in the single and binary systems, (iii) employ four kinetic models including pseudo-first-order, pseudo-second-order, double exponential and intra-particle diffusion for experimental data analysis, (iv) apply the noncompetitive sorption isotherm models (the Langmuir, Freundlich and Dubinin–Radushkevich (D–R)) for equilibrium data analysis in the single system (v) collect the experimental data on sorption equilibrium for the binary system containing Cu(II)-Zn(II) ions, Cu(II)-Co(II) ions and Co(II)-Zn(II) ions; and (vi) study the applicability of the multi-component sorption isotherm models to the simultaneous sorption of the heavy metals in the binary systems.

2. Experimental

2.1. Materials

Nano-sized ZrO_2 powder (the average particle sizes of powder was lower than 15 nm), Pluronic123 (P123) (M_n = 8,400), 3-mercaptopropyltrimethoxysilane (TMPTMS), aminopropyltriethoxylsilane (APTES), PVP (M_n = 1,300,000), ethanol, NaOH and HNO_3 were purchased by Sigma-Aldrich. The solutions of Cu(II), Co(II) and Zn(II) ions were prepared by dissolving weighed amounts of copper, cobalt and zinc nitrates (Aldrich) in deionized water, respectively. Distillated water was used throughout this work.

2.2. Preparation of nanofiber adsorbents

TMPTMS/Zirconia/PVP/P123, APTES/Zirconia/PVP/P123 and APTES/TMPTMS/Zirconia/PVP/P123 solutions were provided by the following method. Briefly, first, the PVP/ethanol/P123 solution prepared by dissolving 0.25 g of surfactant P123 and 1.5 g of PVP to 10 mL ethanol and the mixture was strongly magnetic stirred at 50°C for 6 h. After that, 10 wt% of modified ZrO_2 powder (with the –SH functional groups, $–NH_2$ functional groups or with the –SH/$–NH_2$ bifunctional groups) were dispersed in the PVP/ethanol/P123 solution and then sonicated for 2 h. Then the prepared solution was loaded into the 10 mL syringe. A feed pump of syringe was used to exude the polymer solution at a speed of 0.30 ml/h through a needle with an inner diameter of 0.50 mm and two voltages of 17.5 and 20 kV. The tip-to-collector distance was 15 cm. Under high voltage, a jet was formed and moved to the counter electrode that was covered with aluminum foil. The nanofibers were collected on the aluminum foil. The nanofibers were dried at 50°C for 3 h.

2.3. Nanofiber characterization studies and determination of pH_{pzc}

Fourier transform infrared spectroscopy (FTIR) (Vector22- Bruker Company, Germany) was used to characterize the chemical structure of prepared nanofiber adsorbents in the range of 400–4,000 cm^{-1}. The surface morphology of the electrospun APTES/TMPTMS/Zirconia/PVP/P123 nanofibers was characterized with scanning electron microscopy (SEM, JEOL JSM-6380). Specific surface area, total pore volume and pore size was estimated by the BET and BJH methods. The point of zero charge (PZC) was considered for finding the surface charge of the APTES/TMPTMS/Zirconia/PVP/P123 nanofiber adsorbent. pH_{pzc} was determined by the following method. 25 ml of 0.1 M NaCl solution was transferred in series of flasks; its initial pH was adjusted in the range of 1–7 by using 0.1 M HNO_3 and/or 0.1 M NaOH solutions. Then 0.1 g of APTES/TMPTMS/Zirconia/PVP/P123 nanofiber adsorbent was added to each solution. Then, the solutions were shaken for 24 h in the dark at 25°C, and the final pH of the solutions was measured by using a portable pH meter. Finally, the final pH values were plotted vs. their corresponding initial pH values. From the graphs, the pH_{pzc} values of nanofiber were specified from the points where the initial pH equals the final pH.

2.4. Sorption equilibrium experiments

The behavior of Cu(II), Co(II) and Zn(II) batch sorption onto the TMPTMS/Zirconia/PVP/P123, APTES/Zirconia/PVP/P123 and APTES/TMPTMS/Zirconia/PVP/P123 adsorbents were investigated in the flasks containing 50 mL solution by shaking the flasks at 200 rpm. Batch sorption experiments onto the multi-functionalized nanofiber adsorbents (APTES/TMPTMS/Zirconia/PVP/P123) were investigated under different pH (1–7), temperature of 25°C, initial Cu(II), Co(II) and Zn(II) ion concentration of 100 mg/L (1.573, 1.697, 1.529 mmol/L for Cu(II), Co(II) and Zn(II) ions, respectively), contact time of 240 min with an adsorbent dose of 1 g/L in

the single-component system. In all binary mixtures, for each initial concentration of first metal ion solution (the first metal ion in the Cu(II)-Co(II) and Cu(II)-Zn(II) systems was Cu(II) and in Co(II)-Zn(II) system was Co(II)) viz.: 10, 30, 50, 100, 200, 300 mg/L, the second metal ion solution concentration was varied in the range of 10–300 mg/L (viz., 10, 30, 50, 100, 200, 300 mg/L). The simultaneous sorption experiments were considered at a temperature of 45°C, contact time of 240 min, with an adsorbent dose of 1 g/L and initial pH 6.0 for the sorption of Cu(II) and Co(II) ions and pH 6.5 for the sorption of Zn(II) ions. The concentration of Cu(II), Co(II) and Zn(II) ions before and after equilibrium sorption was measured by using an inductivity coupled plasma atomic emission spectrophotometer (ICP-AES, Thermo Jarrel Ash, Model Trace Scan). The sorption capacity of APTES/TMPTMS/Zirconia/PVP/P123 nanofiber adsorbent for the sorption of Cu(II), Co(II) and Zn(II) ions was calculated from the following equation:

$$q_e = \frac{(C_0 - C_e)V}{m} \quad (1)$$

where q_e is the equilibrium sorption capacity of nanofiber for heavy metal ions (mmol/g), V is the heavy metal ion solution volume (L), m is the amount of added adsorbent (g), C_0, and C_e are the initial and final Cu(II), Co(II) and Zn(II) ions concentrations (mmol/L), respectively.

3. Results and discussion

3.1. Characterization of nanofibers

After modification of nanofibers with functional groups, the FTIR spectra of TMPTMS/Zirconia/PVP/P123, APTES/Zirconia/PVP/P123 and APTES/TMPTMS/Zirconia/PVP/P123 nanofiber adsorbents were shown in Fig. 1. As can be seen, the broad band at 510–700 cm^{-1} was due to the Zr–O–Zr groups in the nanofibers spectra. The band around 1,040–1,120 cm^{-1} was attributed to the C–O stretching of PVP. As shown, the peaks at 1,330, 1,425, 1,715 and 2,949 cm^{-1} were related to the $–CH_3$ groups, C–H bending, C=O bond and C–H stretching in the nanofiber structure, respectively [16]. As shown in the FTIR spectra of TMPTMS/Zirconia/PVP/P123 (Fig. 1(a)), a broad bond of 3,100–3,600 (cm^{-1}) was assigned to the O–H stretching. While in the FTIR spectra of APTES/Zirconia/PVP/P123 (Fig. 1(b)) and APTES/TMPTMS/Zirconia/PVP/P123 (Fig. 1(c)), O–H stretching of the nanofiber is in the range of 3,100–3,450 cm^{-1}. A new weak peak was observed at 2,530 cm^{-1} which was assigned to the –SH groups in the structure of TMPTMS/Zirconia/PVP/P123 (Fig. 1(a)). Two bonds at 1,623 and 3,463 cm^{-1} were corresponded to the $–NH_2$ groups in the structure of APTES/Zirconia/PVP/P123 (Fig. 1(b)). From the FTIR spectra of the APTES/TMPTMS/Zirconia/PVP/P123 (Fig. 1(c)) nanofiber, the introduction of both amine and thiol groups ($–SH/–NH_2$) on the surface of multi-functionalized nanofiber was confirmed.

The SEM image and distribution diameter of APTES/TMPTMS/Zirconia/PVP/P123 nanofiber adsorbents at applied voltages of 15.0 and 20.0 kV were shown in Fig. 2. As shown, at lower voltages (15.0 kV), the strength of electrical

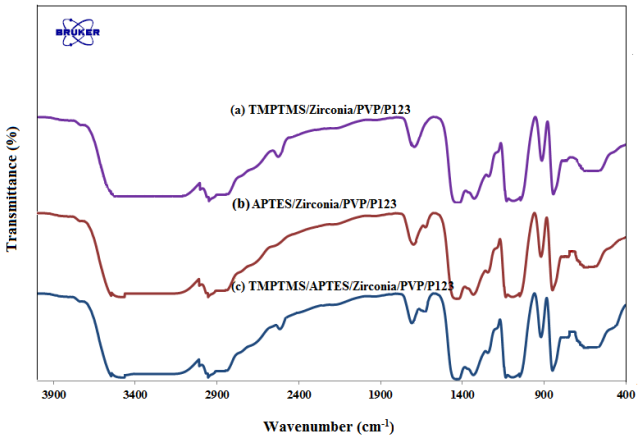

Fig. 1. The FTIR spectra of TMPTMS/ Zirconia/PVP/P123 (a), APTES/Zirconia/PVP/P123 (b) and APTES/TMPTMS/Zirconia/PVP/P123 (c) nanofiber adsorbents.

field was weak for the formation of homogenous fibers and some beads were formed on the aluminum collector. The average fiber diameter was 106.4 nm under applied voltage of 15.0 kV. When the applied voltage increased to 20 kV, the homogeneous fibers (without beads) with average diameter of 98.9 nm were formed on the collector. Based on BJH and BET analyses, S_{BET}, pore volume and average pore diameter of APTES/TMPTMS/Zirconia/PVP/P123 nanofiber adsorbent were 152.60 m^2/g, 0.272 cm^3/g and 2.03 nm, respectively. This indicated that the surface area of nanofiber is high for sorption process. The point of zero charge (pH_{pzc}) value of APTES/TMPTMS/Zirconia/PVP/P123 was obtained 4.6.

3.2. Selection of the best nanofiber adsorbent

The effect of functional groups on nanofibers were investigated for the sorption of Cu(II), Co(II) and Zn(II) ions from aqueous solutions. Experiments were carried out at temperature of 25°C, pH 5.5, adsorbent dosage of 1 g/L and contact time of 300 min by shaking at 200 rpm. The effects of three functional groups (amine groups ($–NH_2$), thiol groups (–SH) and composition of amine groups and thiol groups ($–NH_2/–SH$) on the sorption of heavy metal were shown in Table 1. The results indicated that the sorption capacity of nanofiber adsorbent with multi-functionalized groups (APTES/TMPTMS/Zirconia/PVP/P123) was higher than single-functionalized groups (TMPTMS/Zirconia/PVP/P123 and APTES/Zirconia/PVP/P123). This phenomenon can be due to the more available binding sites such as amine groups, hydroxyl groups and thiol groups with the heavy metal ions. From the FTIR spectra of the APTES/TMPTMS/Zirconia/PVP/P123, presence of these functional groups was confirmed. Therefore, thiol-amine-zirconia-polymer nanofiber adsorbent (APTES/TMPTMS/Zirconia/PVP/P123) was selected to optimize conditions for single and binary sorption of Cu(II), Co(II) and Zn(II) ions from aqueous solutions.

The sorption mechanism of Cu(II), Co(II) and Zn(II) ions (M(II)) on to the multi-functionalized nanofiber adsorbent was shown in Fig. 3. There are three active sites

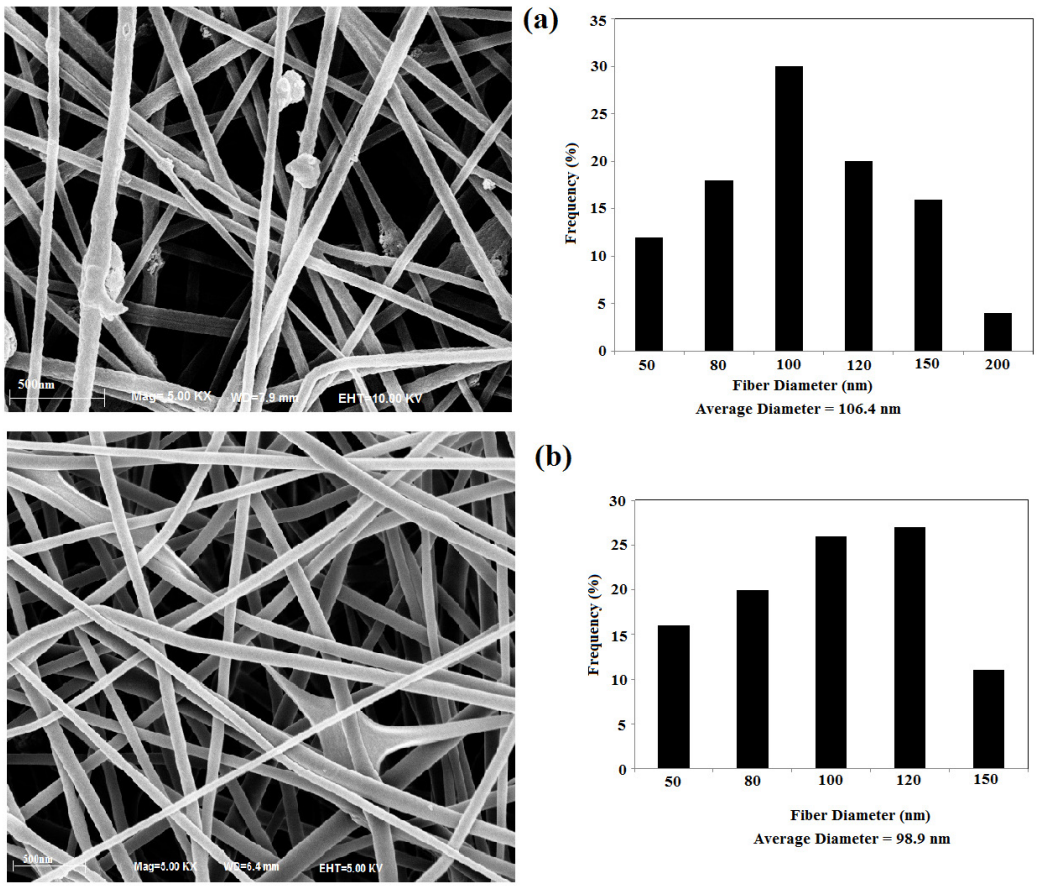

Fig. 2. The SEM image and nanofiber diameter distribution of multi-functionalized zirconia nanofiber adsorbent at applied voltages of 15.0 (a) and 20.0 kV (b).

Table 1
Effect of functional groups on Zirconia nanofibers for the sorption of Cu(II), Co(II) and Zn(II) ions from aqueous solutions

Functional groups	Metal ions	C_0 (mmol/L)	C_e (mmol/L)	q_e (mmol/g)
APTES (–NH_2)	Cu(II)	1.574	0.662	0.912
	Co(II)	1.697	0.857	0.840
	Zn(II)	1.531	1.120	0.411
TMPTMS (–SH)	Cu(II)	1.574	0.651	0.923
	Co(II)	1.697	0.846	0.851
	Zn(II)	1.531	1.108	0.423
APTES-TMPTMS (–NH_2/–SH)	Cu(II)	1.574	0.471	1.103
	Co(II)	1.697	0.787	0.910
	Zn(II)	1.531	1.060	0.471

(OH, SH and NH_2) on the adsorbent which play an important role on sorption process. The sorption mechanism for removal of heavy metal ions from water systems includes ionic interaction between negatively charged polymer adsorbent and positively charged heavy metal ions (M^{2+}) or electron exchange from adsorbent surface to heavy metal ions.

3.3. Effect of pH on the Cu(II), Co(II) and Zn(II) sorption

Heavy metal solution pH plays a significant role in governing the sorption behavior of Cu(II), Co(II) and Zn(II) onto the APTES/TMPTMS/Zirconia/PVP/P123 nanofiber adsorbent. As shown in Fig. 4, the Cu(II), Co(II) and Zn(II) sorption was depended greatly on pH and increased sharply with increasing the pH from 1.0 to 6.0 and was reached a maximum value at pH 6.0 for Cu(II) and Co(II) ions and at pH 6.5 for Zn(II) ion. This fact may be due to the ion exchange of Cu^{2+}, Zn^{2+} and Co^{2+} with H^+ on the APTES/TMPTMS/Zirconia/PVP/P123 nanofiber adsorbent during the sorption process and release of the exchanged hydronium ions to the metal ion solution thereby leading to the decrease of pH values. Increasing the sorption efficiency for pH values between 1 and 6 can be explained by the fact that the ion-exchange interactions exist between the adsorbent and the Cu(II), Co(II) and Zn(II) ions. The dependence of heavy metal sorption on the pH can be described from the perspective of surface chemistry in an aqueous phase. The surface charge of adsorbent is neutral at the zero point of charge pH_{pzc}, while is 4.6 for the APTES/TMPTMS/Zirconia/PVP/P123 nanofiber adsorbent. When pH is lower than the pH_{pzc}, the adsorbent surface is positively charged, and anion sorption occurred by the simple electrostatic attraction. Below the pH_{pzc}, the attraction of protons causes a protonated surface of APTES/

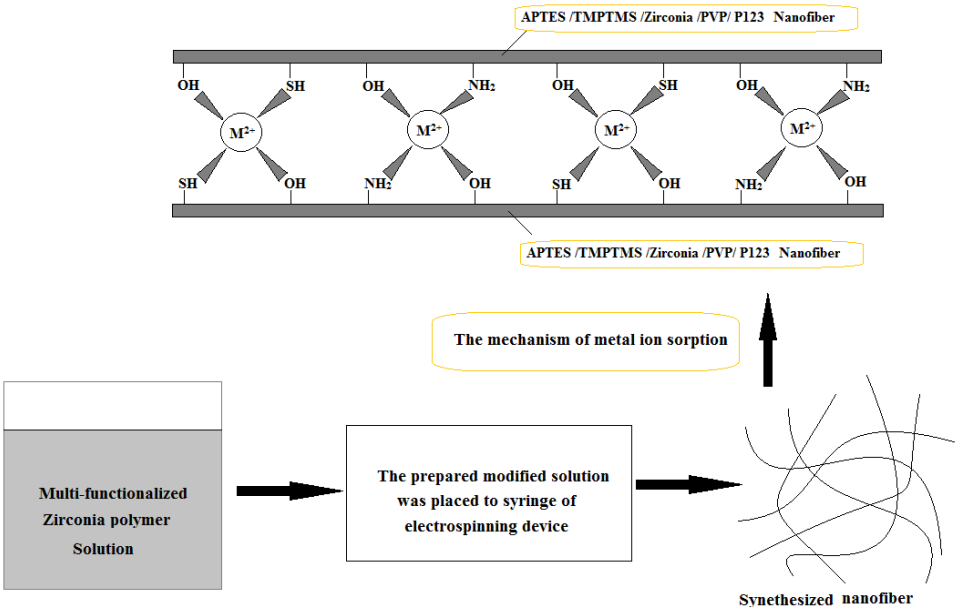

Fig. 3. The mechanism of Cu(II), Co(II) and Zn(II) ions (M(II)) on to the multi-functionalized APTES/TMPTMS/Zirconia/PVP/P123 nanofiber adsorbent.

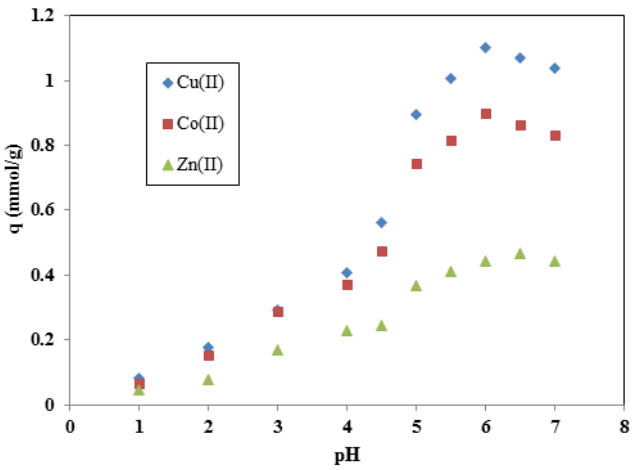

Fig. 4. Effect of solution pH values on the sorption of Cu(II), Co(II) and Zn(II) onto the APTES/TMPTMS/Zirconia/PVP/P123 nanofiber adsorbent (adsorbent dose = 1 g/L, pH = 5, contact time = 240 min T = 25°C).

TMPTMS/Zirconia/PVP/P123 nanofiber adsorbent. There is an electrostatic repulsion between positive charge nanofiber surface and the heavy metal ions (Cu(II), Co(II) and Zn(II)), leading to the lower sorption. Above the pH_{pzc}, the adsorbent surface is negatively charged, and cation sorption occurred. For pH > pH_{PZC}, a release of protons causes a deprotonated APTES/TMPTMS/Zirconia/PVP/P123 nanofiber surface which it causes more attraction of the heavy metal ions onto the surface of nanofiber and increases the sorption capacity. Precipitation usually occurred with the Cu(II), Co(II) and Zn(II) ions attached to hydroxide ions forming $Cu(OH)_2$, $Co(OH)_2$ at pH > 6.0 [20,21] and $Zn(OH)_2$ at pH > 6.5 [22]. Therefore, the nanofiber adsorbent was deteriorated with accumulation of Cu(II), Co(II) and Zn(II) ions and decreased the sorption efficiency of heavy metal ions onto the APTES/TMPTMS/Zirconia/PVP/P123 nanofiber adsorbent.

3.4. Effect of contact time on the Cu(II), Co(II) and Zn(II) sorption

The influence of contact time on the metal ion sorption was considered by varying the time from 0 to 240 min, with an initial concentration of 100 mg/L (1.573, 1.697, 1.529 mmol/L for Cu(II), Co(II) and Zn(II) ions, respectively), at a temperature of 25°C with an optimum pH. The results were shown in Fig. 5. As shown, the sorption process of different heavy metal onto the nanofiber adsorbent reached the equilibrium state after approximately 240 min of contact time. More than 85% of total sorption of Cu(II), Co(II) and Zn(II) ions took place within the first 90 min. According to the experimental results, there were two distinct steps of sorption. The first step of sorption is rapid over the first 90 min, because all active sites on the adsorbents surface were vacant at beginning of process. The second step is slower sorption stage where internal surface diffusion of Cu(II), Co(II) and Zn(II) ions occurs onto the APTES/TMPTMS/Zirconia/PVP/P123 nanofiber adsorbent and the active sites had a tendency to saturate with increasing the contact time in this stage. After 240 min, a lot of active sites of nanofiber became saturated and few active sites were available. Consequently, a contact time of 240 min was selected for further sorption experiments.

3.5. Sorption kinetics

The prediction of kinetics is essential for the design of sorption systems and offers valuable information about the

mechanism of sorption process. The experimental data were analyzed by the non-linear regression using the MATLAB software. The nonlinear equations of these kinetic models are expressed as follows [9,17,23]:

$$\text{Pseudo-first-order: } q_t = q_e\left(1-\exp(-k_1 t)\right) \quad (2)$$

$$\text{Pseudo-second-order: } q_t = \frac{k_2 q_e{}^2 t}{1+k_2 q_e t} \quad (3)$$

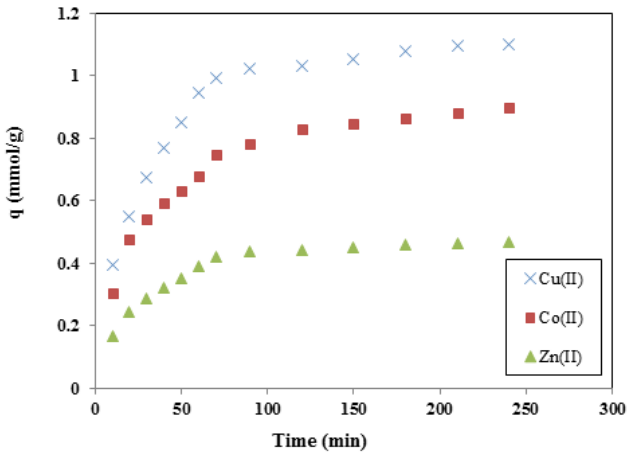

Fig. 5. Effect of contact time on the Cu(II), Co(II) and Zn(II) sorption onto the synthesized zirconia nanofiber adsorbent (adsorbent dose = 1 g/L, pH = 6 for Cu(II) and Co(II) and pH = 6.5 for Zn(II), contact time = 240 min T = 25°C).

$$\text{Double exponential: } q_t = q_e - \frac{D_1}{m_{ads}}\exp(-k_{D1}t) - \frac{D_2}{m_{ads}}\exp(-k_{D2}t) \quad (4)$$

$$\text{Intra-particle-diffusion: } q_t = k_p t^{0.5} + C \quad (5)$$

where q_t and q_e (mmol/g) are the sorption capacity of APTES/TMPTMS/Zirconia/PVP/P123 nanofiber adsorbent at time t and equilibrium, respectively; k_1 (min^{-1}) is the pseudo-first-order rate constant; k_2 (g/(mmol. min)) is the sorption rate constant; k_{D1} and k_{D2} (min^{-1}) are the double exponential rate constant; D_1 and D_2 (g/L) are the equation constants which correspond to the rapid phase and slow phase, respectively; m_{ads} (g/L) is the nanofiber adsorbent concentration; C (mmol/g) is a constant related to the thickness of the boundary layer and k_p (mmol/(g. min)) is the intra-particle diffusion rate constant. The kinetic models parameters; and the correlation coefficient (R^2) of kinetic models were given in Table 2. If C constant in Eq. (5) be near the zero, this line passes through the origin approximately and then intra-particle diffusion will be the rate-controlling step. If the experimental data present multi-linear plots, then, at least two or more steps will effect on the sorption process. The parameters of the kinetic models were determined by the non-linear regression using the MATLAB software and the results of these models were presented in Table 2. As can be seen, by comparing the values of correlation coefficient (R^2) for four kinetic models, namely, pseudo-first-order, pseudo-second-order, double exponential and intra-particle-diffusion models, it was found that the experimental data was best described by the double exponential kinetic model (R^2 > 0.991). This kinetic model describes that the sorption process include

Table 2
Kinetic parameters for the Cu(II), Co(II) and Zn(II) sorption onto the multi-functionalized zirconia nanofiber adsorbent

Metal	q_{exp} (mmol/g)	Pseudo-first-order model			
		K_1 (min^{-1})	q (mmol/g)	RMSE	R^2
Cu(II)	1.102	0.034	1.075	0.032	0.970
Co(II)	0.899	0.032	0.855	0.043	0.949
Zn(II)	0.467	0.034	0.457	0.016	0.964
		Pseudo-second-order model			
		K_2 (g/mmol.min)	q (mmol/g)	RMSE	R^2
Cu(II)	1.102	0.037	1.277	0.031	0.973
Co(II)	0.899	0.043	0.981	0.018	0.980
Zn(II)	0.467	0.087	0.520	0.013	0.983
		Double-exponential kinetic model			
		D_1 (g/L)	K_{D1} (min^{-1})	D_2 (g/L)	K_{D2} (min^{-1})	q (mmol/g)	RMSE	R^2
Cu(II)	1.102	0.038	0.90	0.938	0.028	1.090	0.022	0.994
Co(II)	0.899	0.683	0.02	4.969	2.304	0.886	0.021	0.991
Zn(II)	0.467	3.543	1.373	0.382	0.026	0.465	0.010	0.994
		Intra-particle diffusion			
		K_p (mmol/(g.min))		C (mmol/g)	RMSE	R^2		
Cu(II)	1.102	0.052		0.415	0.105	0.805		
Co(II)	0.899	0.043		0.302	0.063	0.889		
Zn(II)	0.467	0.022		0.176	0.043	0.817		

initial rapid phase which was appertained to the external surface sorption of Cu(II), Co(II) and Zn(II) ions by the nanofiber adsorbents and second step relates to the internal diffusion of these metal ions that the metal ions were adsorbed inside the pores of APTES/TMPTMS/Zirconia/PVP/P123 nanofiber adsorbent. The results showed that the intra-particle diffusion was involved in the Cu(II), Co(II) and Zn(II) ion sorption onto the APTES/TMPTMS/Zirconia/PVP/P123 nanofiber adsorbent, but, this stage of sorption process is not the only rate-controlling mechanism. The intra-particle diffusion model may be consisted of some steps of sorption including external surface sorption, diffusion of Cu(II), Co(II) and Zn(II) ions inside the pores of the nanofiber adsorbent, and final equilibrium stage.

3.6. Effect of concentration of Cu(II), Co(II) and Zn(II) ions

3.6.1. Single component system

The change in the sorption behavior of APTES/TMPTMS/Zirconia/PVP/P123 nanofiber adsorbent with different heavy metal ion concentration from 10 to 500 mg/L (0.157 to 7.868, 0.169 to 8.485 and 0.153 to 7.648 mmol/L for Cu(II), Co(II) and Zn(II) ions, respectively) was shown in Fig. 6. The sorption capacity of APTES/TMPTMS/Zirconia/PVP/P123 nanofiber revealed a highly concentration dependent phenomenon. As can be seen in Fig. 6, the sorption capacity of APTES/TMPTMS/Zirconia/PVP/P123 nanofiber adsorbent for Cu(II), Co(II) and Zn(II) ions increased from 0.124 to 3.116, 0.085 to 2.376 and 0.075 to 1.805 mmol/g at 25°C with increasing the initial concentration of Cu(II), Co(II) and Zn(II) ions, respectively. This uptrend can be due to an increase in the initial ion concentration providing a larger driving force to overcome all mass transfer resistances between the APTES/TMPTMS/Zirconia/PVP/P123 nanofiber adsorbent and the aqueous phase. In particular, at low initial concentration region, the sorption capacity of nanofiber sharply increased with increasing the initial Cu(II), Co(II) and Zn(II) ions concentration because the active sites of APTES/TMPTMS/Zirconia/PVP/P123 nanofiber were enough to react with the heavy metal ions. The temperature influence on the sorption capacity of nanofiber for the sorption of Cu(II), Co(II) and Zn(II) ions was illustrated in Fig. 6. For Cu(II), Co(II) and Zn(II) ions, the sorption capacity increased with a rise in temperature from 25°C to 45°C and it was concluded that the sorption of all metal ions was an endothermic process. With increasing the temperature, the attractive forces between the APTES/TMPTMS/Zirconia/PVP/P123 nanofiber surface and Cu(II), Co(II) and Zn(II) ions became stronger and then sorption increased.

3.6.2. Binary metal ion systems

The simultaneous sorption behavior of metal ions was investigated in three binary systems containing Cu(II)-Zn(II) ions, Cu(II)-Co(II) ions and Co(II)-Zn(II) ions. In binary metal ion systems, the results from simultaneous sorption were shown in Figs. 7–9 for Cu(II)-Zn(II), Cu(II)-Co(II) and Co(II)-Zn(II) systems, respectively. The effect of a competitive ion was examined by varying the initial concentration of one heavy metal ion from 0 to 300 mg/L (0 to 4.721 mmol/L for Cu(II), 0 to 5.090 mmol/L for Co(II) ion and 0 to 4.589 mmol/L for Zn(II) ion). As can be seen in Figs. 7–9, the sorption capacities in the binary systems were lower than those in single systems due to the competition between heavy metal ions to occupy the active sites in the nanofiber adsorbent. The sorption capacity of APTES/TMPTMS/Zirconia/PVP/P123 nanofiber adsorbent for Cu(II), Co(II) and Zn(II) ions increased with increasing the initial concentration of Cu(II), Co(II) and Zn(II) ions up to 4.721, 5.090 and 4.589 mmol/L, respectively. As can be seen in Figs. 7(a) and 8(a), in the Cu(II)-Co(II), Cu(II)-Zn(II) ions systems, Cu(II) was the primary heavy metal ion and Co(II) and Zn(II) were inhibitor ions, and in the binary Co(II)-Zn(II) system (Fig. 9(a)), Co(II) was the primary heavy metal ion and Zn(II) was inhibitor ion. In all systems, the sorption capacity of adsorbent

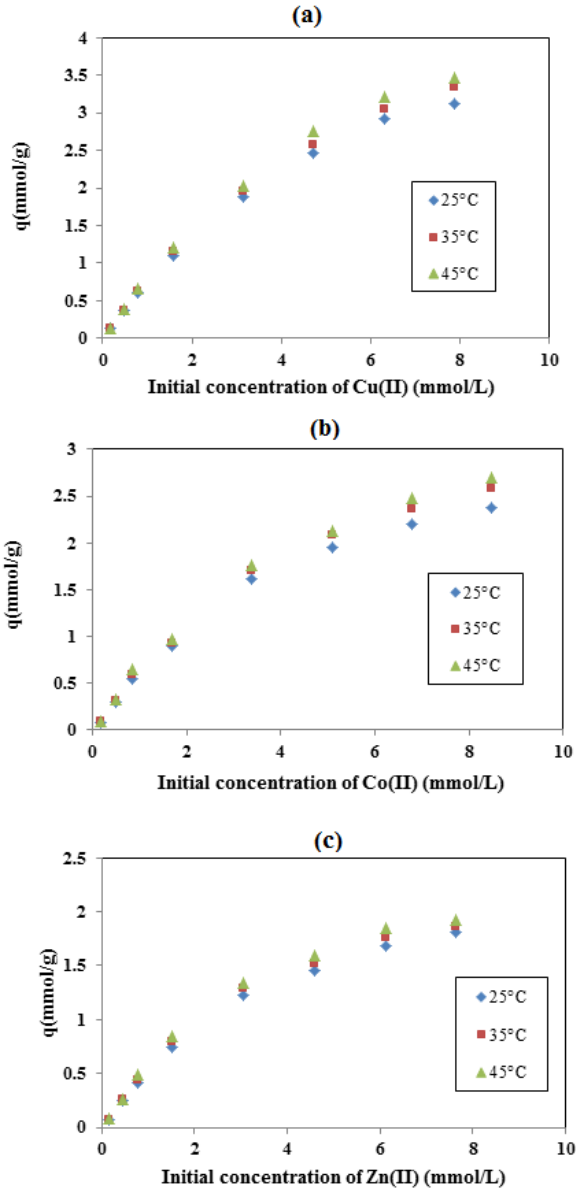

Fig. 6. Effect of initial concentration and temperature on the sorption of Cu(II) (a), Co(II) (b) and Zn(II) (c) onto the APTES/TMPTMS/Zirconia/PVP/P123 nanofiber adsorbent.

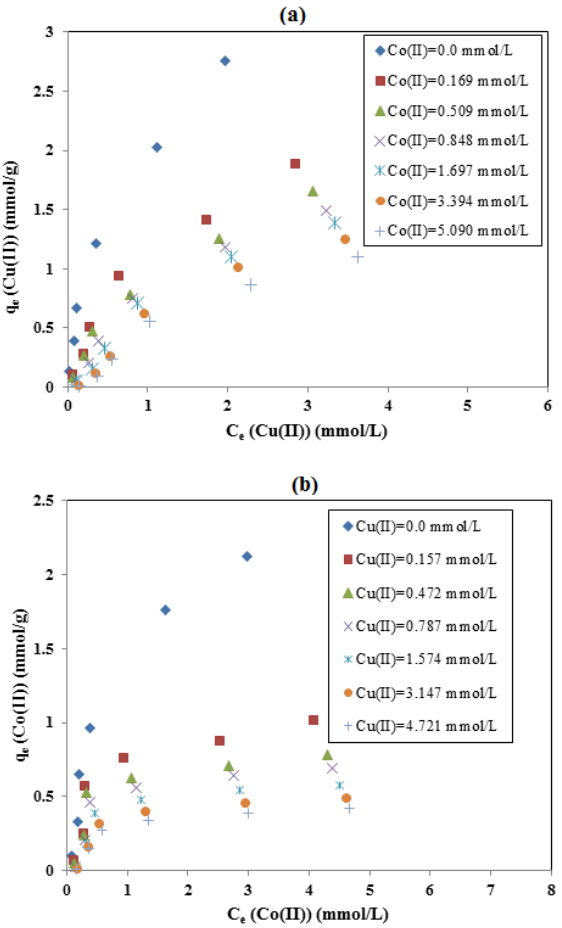

Fig. 7. Comparison of sorption capacity of APTES/TMPTMS/Zirconia/PVP/P123 nanofiber for Cu(II) ion at varying concentrations of Co(II) ion (a) and Comparison of sorption capacity for Co(II) ion at varying concentrations of Cu(II) ion (b).

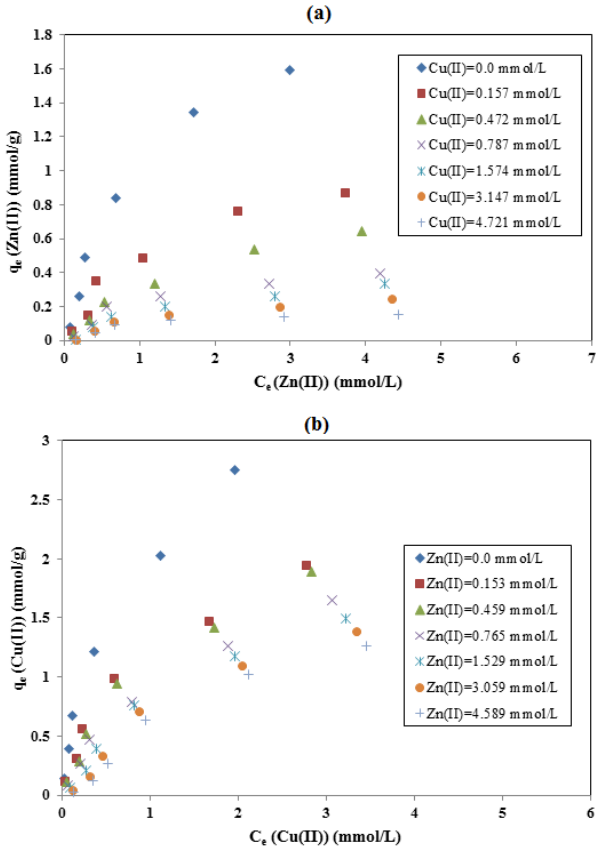

Fig. 8. Comparison of sorption capacity of APTES/TMPTMS/Zirconia/PVP/P123 nanofiber for Cu(II) ion at varying concentrations of Zn(II) ion (a) and Comparison of sorption capacity for Zn(II) ion at varying concentrations of Cu(II) ion (b).

decreased with increasing the inhibitor ions. The presence of inhibitor ions was retarded the equilibrium sorption of primary metal ions onto the nanofiber adsorbents. As can be seen in Figs. 7–9, the both sorption patterns in the single and the binary systems were similar. In the absence of inhibitor ions in the solution, the sorption capacity of nanofiber for primary ion was greater than those in the presence of inhibitor ions. For instance, in the absence of Co(II) ion in the Cu(II)-Co(II) solution, the sorption capacity of nanofiber for Cu(II) ion was 1.212 mmol/g in the initial Cu(II) ion concentration of 100 mg/L (1.574 mmol/L). When the concentration of Co(II) ion was kept at 100 mg/L (1.697 mmol/L) in the solution in the same initial Cu(II)ion concentration, the sorption capacity of adsorbent for Cu(II) ion was decreased to 0.708 mmol/g. As can be seen in Figs. 7(b)–9(b), the binary systems were Co(II)-Cu(II), Zn(II)-Cu(II) and Zn(II)-Co(II), respectively. For instance, in the Co(II)-Cu(II) system, Co(II) was the primary heavy metal ion and Cu(II) was inhibitor ion. As can be seen in Fig. 7(b), in 100 mg/L (1.697 mmo/L) initial Co(II) ion concentration, the adsorbed Co(II) ion at equilibrium were found to be 0.967 and 0.475 mmol/g in the absence of Cu(II) ion and in the presence of 100 mg/L Cu(II) ion concentration, respectively. Comparison of Fig. 7(a), with Fig. 7(b) illustrated that the inhibitory influence of competitive Cu(II) ion on the Co(II) sorption was more significant than the inhibitory influence of competitive Co(II) ion on the Cu(II) sorption. Also, the effect of Cu(II) ions on the Zn(II) sorption capacity was more than the influence of Zn(II) ions on the Cu(II) sorption capacity by comparison of Fig. 7(a) with Fig. 7(b). Furthermore, comparison of Fig. 7(a), with Fig. 7(b) indicated that effect of Co(II) ions on the Zn(II) sorption capacity was more than the influence of Zn(II) ions on the Co(II) sorption capacity. However, the sorption capacity for the binary system appeared to be lowered than that of the single component as the concentration became high.

3.7. Sorption isotherm models

The design of a sorption system needs the use of an appropriate correlation for the equilibrium curves. Consequently, the equilibrium sorption data of Cu(II), Co(II) and Zn(II) ions from single and binary systems onto the APTES/TMPTMS/Zirconia/PVP/P123 nanofiber adsorbent have been used to test the applicability of various mono and multi component isotherm models.

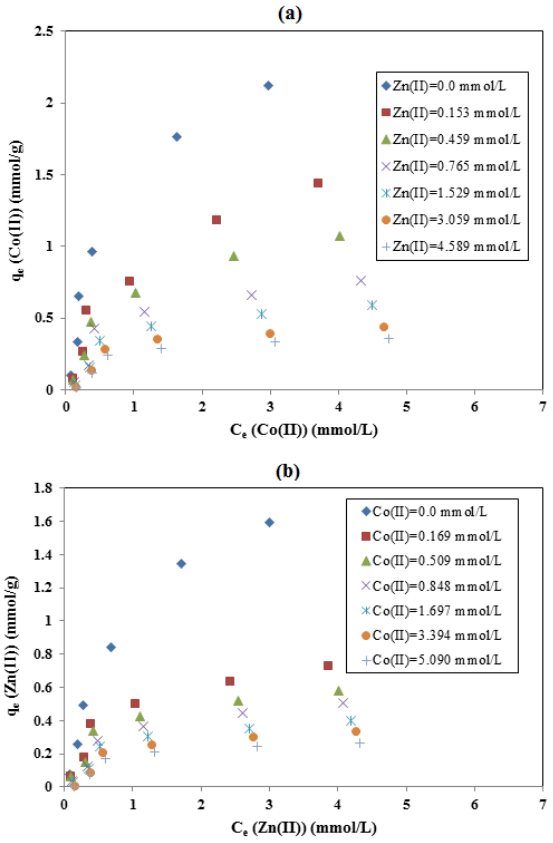

Fig. 9. Comparison of sorption capacity of APTES/TMPTMS/Zirconia/PVP/P123 nanofiber for Co(II) ion at varying concentrations of Zn(II) ion (a) and Comparison of sorption capacity for Zn(II) ion at varying concentrations of Co(II) ion (b).

3.7.1. Single component isotherm models

The sorption equilibrium data for a single component system can be usually explicated by the Langmuir, Freundlich and Dubinin–Radushkevich (D–R) isotherm models. The Langmuir isotherm assumes a monolayer sorption onto a surface of adsorbent containing a finite number of sorption sites of uniform strategies of sorption [24]. The Freundlich isotherm is an empirical equation that is used to explain the multilayer sorption onto the heterogeneous surface of adsorbent. Another popular models used in the analysis of isotherms is that proposed by the Dubinin- Radushkevich (D–R) [24,25]. The D-R model was used to estimate the type of chemical or physical sorption process. These isotherm models are represented mathematically as [17,23,26]:

$$\text{Langmuir isotherm: } q_e = \frac{q_m K_L C_e}{1 + K_L C_e}, \qquad R_L = \frac{1}{1 + K_L C_0} \tag{6}$$

$$\text{Freundlich isotherm: } q_e = K_F C_e^{1/n} \tag{7}$$

D-R isotherm:

$$q_e = q_{DR} \exp(-B_{DR}\varepsilon^2), \quad \varepsilon = RT \ln\left(1 + \frac{1}{C_e}\right), \; E = \frac{1}{\sqrt{2B_{DR}}} \tag{8}$$

where q_m (mmol/g) is the maximum sorption capacity, k_L (L/mmol) Langmuir constants related to the energy of sorption, q_e (mmol/g) is the sorption capacity at equilibrium, C_e (mmol/L) is the equilibrium concentration of the adsorbate; the R_L values examine the types of isotherm: irreversible isotherm (R_L = 0), favorable isotherm (0 < R_L < 1), linear isotherm (R_L = 1) and unfavorable isotherm (R_L > 1) [26]. In $R_L = 1/1 + K_L C_0$ equation, C_0 (mmol/L) is the highest initial solute concentration [17]. The parameters of n and K_f ((mmol/g)/(l/mmol)$^{1/n}$) are the Freundlich isotherm constants which are related to the intensity of the sorption and sorption capacity, respectively. Values of n greater than 1 indicate the favorable nature of sorption [26]. The parameter of q_{DR} is the theoretical isotherm saturation capacity (mmol/g), B_{DR} is the activity coefficient related to adsorption free energy (mol^2/J^2) and ε_{DR} is the Polanyi potential. R and T are the gas constant (8.314 J/(mol. K)) and absolute temperature (K), respectively. The mean free energy of sorption (E (KJ/mol)) was used to estimate the type of chemical or physical sorption process. If 1 < E (kJ/mol) < 8, the physical sorption becomes a dominant mechanism and if 8 < E (kJ/mol) < 16, the sorption reaction can be explained by a chemical sorption mechanism [23]. Furthermore, the residual root mean square errors (RMSE) and the correlation coefficient (R^2) of isotherm models were used to measure the goodness of fit. RMSE is defined as [16]:

$$\text{RMSE} = \sqrt{\left(\frac{1}{n-2}\right)\sum_{i=1}^{n}\left(q_{i,\text{exp}} - q_{i,\text{cal}}\right)^2} \tag{9}$$

where $q_{i,\text{cal}}$ and $q_{i,\text{exp}}$ (mmol/g) are the calculated and the experimental values of the sorption capacity, respectively, and n is the number of data points. A smaller RMSE value indicates a better curve fitting. Parameters of single isotherm models at different temperatures were given in Table 3. Higher correlation coefficients and smaller RMSE values indicated that the Langmuir model fits the sorption data better than Freundlich and D-R model because of the homogeneous distribution of active sites on the APTES/TMPTMS/Zirconia/PVP/P123 nanofiber adsorbent. Furthermore, q_m of adsorbent for Cu(II), Co(II) and Zn(II) ions increased with increasing the temperature. As can be seen in Table 3, the values of K_L increased from 0.799 to 1.044 for Cu(II) ion, 0. 590 to 0.958 for Co(II) ion and 0.601 to 0.784 for Zn(II) ion with a rise in temperature from 25°C to 45°C. The values of R_L are in the range of 0–1 which indicates the favorable sorption. The values of n (Table 3) were all between 1 and 10, indicated that the sorption was favorable. The values of E were found to be 1–8 KJ/mol, and they were in the range of values for physical sorption for all heavy metal ions.

In Table 4, the maximum sorption capacity of APTES/TMPTMS/Zirconia/PVP/P123 nanofiber adsorbent for Cu(II), Co(II) and Zn(II) ions was compared with that of the other adsorbents reported in the literature. As can be seen in Table 4, the maximum sorption capacity of adsorbent was in the range of maximum sorption capacity of other adsorbents for Cu(II), Co(II) and Zn(II) ions obtained by the other researchers.

Table 3
Langmuir, Freundlich and Dubinin–Radushkevich parameters for the Cu(II), Co(II) and Zn(II) sorption onto the multi-functionalized nanofiber adsorbent in the single component system

Metal	Temperature °C	Langmuir isotherm				
		q_m (mmol/g)	K_L (L/mmol)	R_L	RMSE	R^2
Cu(II)	25	3.928	0.799	0.209	0.063	0.998
	35	4.126	0.847	0.200	0.091	0.996
	45	4.146	1.044	0.167	0.132	0.991
Co(II)	25	3.032	0.590	0.249	0.056	0.997
	35	3.034	0.808	0.196	0.087	0.993
	45	3.050	0.958	0.170	0.137	0.985
Zn(II)	25	2.299	0.601	0.266	0.027	0.998
	35	2.320	0.685	0.241	0.035	0.998
	45	2.352	0.784	0.217	0.052	0.996
		Freundlich isotherm				
		K_F (mmol/g)	n	RMSE		R^2
Cu(II)	25	1.556	2.041	0.169		0.971
	35	1.682	2.047	0.153		0.974
	45	1.862	2.177	0.174		0.972
Co(II)	25	1.024	1.990	0.170		0.959
	35	1.166	2.094	0.181		0.960
	45	1.255	2.166	0.189		0.969
Zn(II)	25	0.784	1.975	0.114		0.965
	35	0.843	2.040	0.127		0.961
	45	0.910	2.113	0.144		0.956
		Dubinin-Radushkevich isotherm				
		q_{DR} (mmol/g)	B_{DR} (mol^2/J^2)*10^8	E (KJ/mol)	RMSE	R^2
Cu(II)	25	2.893	11.30	2.103	0.290	0.949
	35	3.062	10.20	2.214	0.328	0.941
	45	3.142	7.13	2.648	0.356	0.937
Co(II)	25	2.211	17.10	1.802	0.218	0.949
	35	2.320	9.78	2.261	0.202	0.956
	45	2.390	7.43	2.594	0.240	0.951
Zn(II)	25	1.671	16.12	1.761	0.148	0.958
	35	1.728	13.20	1.946	0.152	0.960
	45	1.782	10.28	2.205	0.159	0.952

3.7.2. Binary-component sorption isotherm models

The binary-component sorption isotherms are normally attained by extending the above single component sorption isotherm models. The following binary component sorption isotherm models have been used in this investigation:

- The Non-modified Langmuir Binary component Isotherm (NLBI) model. This model is the extension of the single component Langmuir model. NLBI model is represented mathematically as follows [34]:

$$q_{e,1} = \frac{q_{m,1} K_{L,1} C_{e,1}}{1 + K_{L,1} C_{e,1} + K_{L,2} C_{e,2}}, \quad q_{e,2} = \frac{q_{m,2} K_{L,2} C_{e,2}}{1 + K_{L,1} C_{e,1} + K_{L,2} C_{e,2}}, \qquad (10)$$

where $q_{e,1}$ and $q_{e,2}$ (mmol/g) are the equilibrium solid phase concentration of component 1 and 2 in the binary mixture, respectively; $q_{m,1}$ and $q_{m,2}$ (mmol/g) are the maximum sorption capacity of nanofiber adsorbent for component 1 and 2 in the binary mixture, respectively; $C_{e,1}$ and $C_{e,2}$ (mmol/L) are the un-adsorbed concentration of component 1 and 2 in the binary mixture at equilibrium, respectively; $K_{L,1}$ and $K_{L,2}$ are the individual Langmuir isotherm constant of each component 1 and 2 in the binary mixture (L/mmol), respectively.

- The Modified Langmuir Binary-component Isotherm (MLBI). This model, based on the mechanism of direct competition for the sorption sites, is one of the most widely used models because the isotherm parameters of single-component models may not explain exactly the binary-component sorption behavior of heavy metal ions. An interaction term, $\eta_{L,i}$, is used in the MLBI model which is a characteristic of each species and depends on the concentrations of the other components [35,36]. MLBI model is given as [36]:

Table 4
Comparison of maximum sorption capacity of synthesized adsorbent for the Cu(II), Co(II) and Zn(II) sorption with other adsorbents reported in the literature

Adsorbent	Adsorbent dose (g/L)	$q_{m,Cu(II)}$ (mmol/g)	$q_{m,Co(II)}$ (mmol/g)	$q_{m,Zn(II)}$ (mmol/g)	References
Chitin nanofibrils	1	2.22	–	2.060	[1]
Carbon nanotubes	5	0.0549	0.044	–	[2]
Acetate/zeolite composite fiber	4	0.460	–	–	[11]
Graphene oxide	0.07	–	–	3.763	[22]
PVA/ZnO nanofiber	1	2.557	–	–	[23]
Nanoporous carbon	0.5	–	–	2.0	[27]
Commercial activated carbon	0.5	–	–	0.625	[27]
Keratin/PA6 blend nanofibres	1	1.629	–	–	[28]
Meso-HA nanofibers	0.8	–	1.47×10^{-4}	–	[29]
Chitosan/HAp composite nanofiber	1	–	3.057	–	[30]
Chitosan/clinoptilolite	10	11.32	7.939	–	[31]
Functionalized polymer	1	1.201	–	–	[32]
Anatase mesoporous titanium nanofibers	2.5	0.201	–	–	[33]
APTES/TMPTMS/Zirconia/PVP/P123 nanofiber	1	4.146	3.050	2.352	This work

$$q_{e,1} = \frac{q_{m,1}K_{L,1}(C_{e,1}/\eta_{L,1})}{1+K_{L,1}(C_{e,1}/\eta_{L,1})+K_{L,2}(C_{e,2}/\eta_{L,2})},$$
$$q_{e,2} = \frac{q_{m,2}K_{L,2}(C_{e,2}/\eta_{L,2})}{1+K_{L,1}(C_{e,1}/\eta_{L,1})+K_{L,2}(C_{e,2}/\eta_{L,2})} \quad (11)$$

where $\eta_{L,1}$ and $\eta_{L,2}$ (dimensionless) are the binary-component Langmuir sorption constant of component 1 and 2 in the binary mixture, respectively.

- The Extended Freundlich Binary-component Isotherm (EFBI). EFBI model is given as [19]:

$$q_1 = \frac{K_{F,1}C_1^{\left(\frac{1}{n_1}\right)+x_1}}{C_1^{x_1}+y_1C_2^{z_1}}, \quad q_2 = \frac{K_{F,2}C_2^{\left(\frac{1}{n_2}\right)+x_2}}{C_2^{x_2}+y_2C_1^{z_2}}, \quad (12)$$

where $K_{F,1}$ and $K_{F,2}$ ((mmol/g)/(L/mmol)$^{1/n}$) are the individual Freundlich isotherm constant of component 1 and 2 in the binary mixture, respectively; the other six parameters (x_1; y_1; z_1 and x_2; y_2; z_2) are the binary-component Freundlich sorption constants of the first and the second components and n_1 and n_2 can be estimated from the analogous individual Freundlich isotherm models.

- The Sheindorf–Rebuhn–Sheintuch Isotherm (SRSI). The competition coefficients a_{ij} in the SRS model investigate the sorption inhibitory effect of component i by component j. The general SRS equation for component 1 and 2 in a binary component system is given as [37]:

$$q_{e,1} = K_{F,1}C_{e,1}\left(a_{11}C_{e,1}+a_{12}C_{e,2}\right)^{\left(\frac{1}{n_1}\right)-1}$$
$$q_{e,2} = K_{F,2}C_{e,2}\left(a_{21}C_{e,1}+a_{22}C_{e,2}\right)^{\left(\frac{1}{n_2}\right)-1} \quad (13)$$

where a_{11} = a_{22} = 1; a_{12} (dimensionless) is the competition coefficients of component 1 by component 2 and a_{21} (dimensionless) is the competition coefficients of component 2 by component 1. Table 5 showed the parametric values of all the binary component isotherm models and the RMSE values between the experimental and calculated q_e values. Table 5 revealed that the experimental data fitted poorly with the binary-component NLBI model (RMSE = 0.2364, 0.1971 and 0.1460 for Cu(II)-Co(II), Cu(II)-Zn(II) and Co(II)-Zn(II) systems, respectively). A comparison between all interaction terms ($\eta_{L,1}$ and $\eta_{L,2}$) in the MLBI model illustrated that the level of interaction terms were greater than 1 indicating that the NLBI model related to the individual isotherm parameters could not be used to estimate the binary-system sorption. One of reason is that this model does not incorporate any parameter accounting for the interactions between heavy metal ions of different species and competition among metal cations. For the sake of comparison, according to the experimental data analyses, the maximum sorption capacity of APTES/TMPTMS/Zirconia/PVP/P123 nanofiber adsorbent in the single system was higher than those in the binary systems. The fitting of the MLBI model was slightly improved by using of the η terms. Also, the Freundlich-type isotherm models: EFBI and SRSI models were tested for predicting the sorption behavior of heavy metal ions in the binary systems. As can be seen in Table 5, based on RMSE values, the EFBI fitted the experimental data marginally better than the SRSI because the RMSE of EFBI was lower than that of the SRSI for the all binary metal-nanofiber systems. As an example, for the Cu(II)-Co(II) system, RMSE of EFBI was 0.1137, whereas that of SRSI was 0.0960. The estimated competition coefficients a_{12} and a_{21} were obtained from the competitive sorption data by using MATLAB software. As can be seen in Table 5, in the binary Cu(II)-Co(II) system (Cu(II) as primary metal ion and Co(II) as secondary meal ion), a_{12} and a_{21} were found to be 90.070 and 1.277 which indicated that the inhibitory effect of competitive Cu(II) ion on the Co(II) sorption was greater than the inhibitory effect of competitive Co(II) ions on the

Table 5
Binary-component isotherm parameter values for the simultaneous sorption of Cu(II), Co(II) and Zn(II) onto the synthesized Zirconia nanofiber adsorbent

Binary metal systems	Non-modified Langmuir binary component isotherm (NLBI)						
	$q_{m,1}$ (mmol/g)	$q_{m,2}$ (mmol/g)			RMSE		
Cu(II)-Co(II) system (Cu = 1,Co = 2)	2.642	1.075			0.2364		
Cu(II)-Zn(II) system (Cu = 1,Zn = 2)	2.654	1.412			0.1971		
Co(II)-Zn(II) system (Co = 1,Zn = 2)	2.299	0.714			0.1460		
	Modified Langmuir binary-component isotherm (MLBI)						
	$q_{m,1}$ (mmol/g)	$\eta_{L,1}$	$q_{m,2}$ (mmol/g)	$\eta_{L,2}$	RMSE		
Cu(II)-Co(II) system (Cu = 1,Co = 2)	2.642	1.765	0.926	3.362	0.1030		
Cu(II)-Zn(II) system (Cu = 1,Zn = 2)	2.654	1.131	1.417	4.676	0.0486		
Co(II)-Zn(II) system (Co = 1,Zn = 2)	2.299	1.369	0.977	3.752	0.0559		
	Extended Freundlich binary-component isotherm (EFBI)						
	x_1	y_1	z_1	x_2	y_2	z_2	RMSE
Cu(II)-Co(II) system (Cu = 1,Co = 2)	0.259	1.895	0.343	0.703	2.718	0.450	0.0960
Cu(II)-Zn(II) system (Cu = 1,Zn = 2)	0.216	1.403	0.361	0.924	12.71	0.682	0.0485
Co(II)-Zn(II) system (Co = 1,Zn = 2)	0.201	2.383	0.639	0.712	3.251	0.455	0.0521
	Sheindorf–Rebuhn–Sheintuch isotherm (SRSI)						
	a_{11}	a_{12}	a_{21}	a_{22}	RMSE		
Cu(II)-Co(II) system (Cu = 1,Co = 2)	1.00	90.070	1.277	1.00	0.1137		
Cu(II)-Zn(II) system (Cu = 1,Zn = 2)	1.00	16.340	2.127	1.00	0.0510		
Co(II)-Zn(II) system (Co = 1,Zn = 2)	1.00	21.240	1.469	1.00	0.0620		

Cu(II) sorption. In the binary Cu(II)-Zn(II) system (Cu(II) as primary heavy metal and Zn(II) as secondary metal ion), a_{12} and a_{21} values revealed that the sorption capacity for Cu(II) ion was less affected by the presence of Zn(II) ion (a_{12} = 16.340) in comparison to the inhibition employed in the reverse condition (a_{21} = 2.127). In binary Co(II)-Zn(II) system (Co(II) as primary heavy metal and Zn(II) as secondary meal ion), a_{12} and a_{21} were found to be 21.240 and 1.469 which indicated that the effect of Co(II) ions on the Zn(II) sorption capacity was more than the influence of Zn(II) ions on the Co(II) sorption capacity.

The equilibrium data indicated that the potential of the sorption for the metal ions on the APTES/TMPTMS/Zirconia/PVP/P123 nanofiber adsorbent was in order of Cu(II) > Co(II) > Zn(II). This order of heavy metal ion sorption can be justified with the covalent index which can be calculated from the following equation [38]:

$$\text{Covalent index} = X_m^2 r \tag{14}$$

where r and X_m are atomic radius and electronegativity, respectively. When covalent index for a metal is high, the tendency of adsorbent for sorption of that metal from water system is greater than other metal ions with lower covalent index. Based on atomic radius and electronegativity of all three metal ions, covalent index was found to be 462.080, 441.800 and 364.815 for Cu(II), Co(II) and Zn(II), respectively. According to the covalent index values, the order of metal ion sorption was as follows: Cu(II) > Co(II) > Zn(II).

3.8. Thermodynamic parameters

The sorption process was studied at different temperatures (25°C, 30°C, 35°C, 40°C and 45°C). The sorption

dependency on temperature was evaluated from the linearized Van't Hoff equation, Eq. (20) [39]. In general, the Gibbs energy depends on temperature and pressure. This dependence is given by the following expression:

$$G = G(T, P) \tag{15}$$

Based on mathematical and differential equation, we have:

$$dG = \left(\frac{\partial G}{\partial T}\right)_P dT + \left(\frac{\partial G}{\partial P}\right)_T dP \tag{16}$$

When temperature (T) differs slightly from standard state temperature (T_0), free energy change at T can be evaluated as follows (the pressure is constant):

$$\Delta G = \Delta G^\circ(T_0) + \left(\frac{\partial \Delta G^\circ}{\partial T}\right)_P \left[T - T_0\right] \tag{17}$$

Based on Maxwell equation, we have:

$$\left(\frac{\partial \Delta G^\circ}{\partial T}\right)_P = -\Delta S^\circ \tag{18}$$

Hence, Eq. (17) can be simplified to:

$$\Delta G^\circ(T, P) = \Delta G^\circ(T_0) + (-\Delta S^\circ)\left[T - T_0\right] = \left(\Delta G^\circ(T_0) + T_0 \Delta S^\circ\right) - T\Delta S^\circ \tag{19}$$

Since $\Delta H^\circ = \Delta G^\circ(T_0) + T_0 \Delta S^\circ$, consequently, Gibbs energy change is determined by using the following equation [40,41]:

$$\Delta G^\circ = \Delta H^\circ - T\Delta S^\circ \tag{20}$$

On the other hand, the standard Gibbs free energy of sorption is as follows [40,41]:

$$\Delta G^\circ = -RT \ln K_C \tag{21}$$

where R (8.3145 J/(mol. K)) is the ideal gas constant, T (K) is the absolute temperature and K is the thermodynamic equilibrium constant. This constant can be calculated by the following equations [9].

$$K_c = \lim_{C_{el} \to 0} \frac{C_{es}}{C_{el}} \tag{22}$$

where C_{el} (mmol/L) is the equilibrium concentration of Cu(II), Co(II) and Zn(II) ions in the liquid phase and C_{es} (mmol/L) is the equilibrium concentration of these metal ions in the solid phases. The relationship between the equilibrium constant (K_c) and temperature is given by the Van't Hoff equation [39,42,43]:

$$\ln(K_c) = \frac{\Delta S^\circ}{R} - \frac{\Delta H^\circ}{R} \times \frac{1}{T} \tag{23}$$

In general, physical sorption includes an enthalpy change between 2 and 21 kJ/mol, while the enthalpy change of chemisorption falls within the range 80–200 kJ/mol [44]. The free energy change for physical sorption is between –20 and 0 KJ/mol and for chemisorption is between –80 and –400 (KJ/mol) [45]. The values obtained from mentioned equations were listed in Table 6. As shown, all the ΔG° values were negative. For instance, the values of ΔG° changed from –2.79 to –4.08 KJ/mol indicating that the sorption of Cu(II) onto the synthesized nanofiber adsorbent was spontaneous and was in the ranges of the physisorption mechanism. The degree of spontaneity of the reaction increased with increasing the temperature of all three Cu(II), Co(II) and Zn(II) ions which confirms the sorption was favorable at higher temperatures. As can be seen in Table 6, the values of enthalpy changes (ΔH°) and entropy changes (ΔS°) were positive indicates that the process was endothermic and that, during the sorption process, randomness increased at the solid–solution interface. The positive values of ΔH° suggest that a large amount of heat was consumed to transfer the Cu(II), Co(II) and Zn(II) ions from the aqueous into the solid phase. ΔH° values falls within the range 2–21 kJ/mol claiming that physisorption was dominant mechanism. The ΔS° values were positive in all heavy metal ions implying that the dissociative mechanism was involved in the sorption process [9].

Table 6
Thermodynamic parameters for the sorption of Cu(II), Co(II) and Zn(II) onto the APTES/TMPTMS/Zirconia/PVP/P123 nanofiber adsorbent

Parameter	Temperature	Metal ions		
		Cu(II)	Co(II)	Zn(II)
K_c	25°C	3.082	1.389	1.109
	30°C	3.237	1.512	1.170
	35°C	3.546	1.767	1.228
	40°C	4.080	1.894	1.296
	45°C	4.678	2.104	1.376
ΔG° (J/mol)	25°C	–2,788.70	–814.09	–256.33
	30°C	–2,959.10	–1,041.49	–395.51
	35°C	–3,241.40	–1,457.77	–525.94
	40°C	–3,659.06	–1,662.05	–674.73
	45°C	–4,079.12	–1,966.60	–843.87
ΔH° (J/mol)		1,6736.91	1,6643.80	8,403.79
ΔS° (J/mol.K)		63.79	58.55	29.04

4. Conclusion

An electrospun APTES/TMPTMS/Zirconia/PVP/P123 nanofiber adsorbent was prepared for the sorption of Cu(II), Co(II) and Zn(II) ions from aqueous solutions. In the single component systems, contact time of 240 min, pH 6.0 for Cu(II) and Co(II) ions and pH 6.5 for Zn(II) ion and temperature of 45°C were optimum conditions for the sorption of metal ions in the batch system. The FTIR results confirmed that the APTES/TMPTMS/ZrO_2/PVP/P123 nanofiber was functionalized with both amine and thiol groups. The SEM analysis indicated that the average homogenous fiber diameter was 98.7 nm. Based on kinetic results, the experimental data was best described by the double exponential kinetic model

(R^2 > 0.998). Based on Langmuir isotherm modeling, the maximum sorption capacity of APTES/TMPTMS/Zirconia/PVP/P123 nanofiber for Cu(II), Co(II) and Zn(II) ions were found to be 4.146, 3.050 and 2.352 mmol/g, respectively. Thermodynamic parameters approved the feasibility of the process and the spontaneous nature of the sorption process. In the binary Cu(II)-Zn(II) and Cu(II)-Co(II) mixtures, the affinity of the nanofiber adsorbent for Cu(II) ions was greater than that for Zn(II) and Co(II) ions under the same experimental conditions. In the binary Co(II)-Zn(II) mixtures the affinity of the adsorbent for Co(II) ions was greater than that for Zn(II). The equilibrium data indicated that the selectivity order of metal ions sorption on to the synthesized adsorbent was Cu(II)>Co(II)>Zn(II).

References

[1] D. Liu, Y. Zhu, Z. Li, D. Tian, L. Chen, P. Chen, Chitin nanofibrils for rapid and efficient removal of metal ions from water system, Carbohydr. Polym., 98 (2013) 483–489.

[2] A. Stafiej, K. Pyrzynska, Adsorption of heavy metal ions with carbon nanotubes, Sep. Purif. Technol., 58 (2007) 49–52.

[3] A.F. Ngomsik, A. Bee, D. Talbot, G. Cote, Magnetic solid–liquid extraction of Eu(III), La(III), Ni(II) and Co(II) with maghemite nanoparticles, Sep. Purif. Technol., 86 (2012) 1–8.

[4] A. Shafaei, E. Pajootan, M. Nikazar, M. Arami, Removal of Co (II) from aqueous solution by electrocoagulation process using aluminum electrodes, Desalination, 279 (2011) 121–126.

[5] F.L. Becker, D. Rodriguez, M. Schwab, Magnetic removal of cobalt from waste water by ferrite coprecipitation, Proc. Mater. Sci., 1 (2012) 644–650.

[6] F. Pepe, B. Gennaro, P. Aprea, D. Caputo, Natural zeolites for heavy metals removal from aqueous solutions: modeling of the fixed bed Ba^{2+}/Na^{+} ion-exchange process using a mixed phillipsite/chabazite-rich tuff, Chem. Eng. J., 219 (2013) 37–42.

[7] C. Cojocaru, G.Z. Trznadel, A. Jaworska, Removal of cobalt ions from aqueous solutions by polymer assisted ultrafiltration using experimental design approach. Part 1: optimization of complexation conditions, J. Hazard. Mater., 169 (2009) 599–609.

[8] S.E. Bailey, T.J. Olin, R.M. Bricka, D. Adrian, A review of potentially low-cost sorbents for heavy metals, Water Res., 33 (1999) 2469–2479.

[9] S. Abbasizadeh, A.R. Keshtkar, M.A. Mousavian, Sorption of heavy metal ions from aqueous solution by a novel cast PVA/TiO_2 nanohybrid adsorbent functionalized with amine groups, J. Ind. Eng. Chem., 20 (2014) 1656–1664.

[10] D. Liu, Z. Li, W. Li, Z. Zhong, J. Xu, J. Ren, Z. Ma, Adsorption behavior of heavy metal ions from aqueous solution by soy protein hollow microspheres, Ind. Eng. Chem. Res., 52 (2013) 11036–11044.

[11] F. Ji, C. Li, B. Tang, J. Xu, G. Lu, P. Liu, Preparation of cellulose acetate/zeolite composite fiber and its adsorption behavior for heavy metal ions in aqueous solution, Chem. Eng. J., 209 (2012) 325–333.

[12] D. Liu, Y. Zhu, Z. Li, D. Tian, L. Chen, P. Chen, Chitin nanofibrils for rapid and efficient removal of metal ions from water system, Carbohydr. Polym., 98 (2013) 483–489.

[13] J. Beheshtian, A. Ahmadi Peyghan, Z. Bagheri, Formaldehyde adsorption on the interior and exterior surfaces of CN nanotubes, Struct. Chem., 24 (2013) 1331–1337.

[14] F. Ji, C. Li, J. Xu, P. Liu, Dynamic adsorption of Cu(II) from aqueous solution by zeolite/cellulose acetate blend fiber in fixed-bed, Colloids Surfaces A, 434 (2013) 88–94.

[15] L.A. Rodrigues, L.J. Maschio, R.E. da Silva, M.L. C.P. da Silva, Adsorption of Cr(VI) from aqueous solution by hydrous zirconium oxide, J. Hazard. Mater., 173 (2010) 630–636.

[16] S. Yari, S. Abbasizadeh, S.E. Mousavi, Adsorption of Pb(II) and Cu(II) ions from aqueous solution by an electrospun CeO_2 nanofiber adsorbent functionalized with mercapto groups, Process Safe Environ. Protect., 94 (2015) 159–171.

[17] S. Abbasizadeh, A.R. Keshtkar, M.A. Mousavian, Preparation of a novel electrospun polyvinyl alcohol/titanium oxide nanofiber adsorbent modified with mercapto groups for uranium(VI) and thorium(IV) removal from aqueous solution, Chem. Eng. J., 220 (2013) 161–171.

[18] M. Teng, H. Wang, F. Li, B. Zhang, Thioether-functionalized mesoporous fiber membranes: sol–gel combined electrospun fabrication and their applications for Hg^{2+} removal, J. Colloid Interface Sci., 355 (2011) 23–28.

[19] V.C. Srivastava, I.D. Mall, I.M. Mishra, Competitive adsorption of cadmium(II) and nickel(II) metal ions from aqueous solution onto rice husk ash, Chem. Eng. Process., 48 (2009) 370–379.

[20] M. Kara, H. Yuzer, E. Sabah, M.S. Celik, Adsorption of cobalt from aqueous solutions onto sepiolite, Water Res., 37 (2003) 224–232.

[21] M.V. Wan, C.C. Kan, B.D. Rogel, M.L.P. Dalida, Adsorption of copper (II) and lead (II) ions from aqueous solution on chitosan-coated sand, Carbohydr. Polym., 80 (2010) 891–899.

[22] H. Wang, X. Yuan, Y. Wu, H. Huang, G. Zeng, Y. Liu, X. Wang, N. Lin, Y. Qi, Adsorption characteristics and behaviors of graphene oxide for Zn(II) removal from aqueous solution, Appl. Surf. Sci., 279 (2013) 432–440.

[23] H. Hallaji, A.R. Keshtkar, M.A. Moosavian, A novel electrospun PVA/ZnO nanofiber adsorbent for U(VI), Cu(II) and Ni(II) removal from aqueous solution, J. Taiwan Inst. Chem. Eng., 46 (2015) 109–118.

[24] V.K. Gupta, D. Pathania, S. Sharma, P. Singh, Preparation of bio-based porous carbon by microwave assisted phosphoric acid activation and its use for adsorption of Cr(VI), J. Colloid Interface Sci., 401 (2013) 125–132.

[25] M. Yari, M. Rajabi, O. Moradi, A. Yari, M. Asif, S. Agarwal, V.K. Gupta, Kinetics of the adsorption of Pb(II) ions from aqueous solutions by graphene oxide and thiol functionalized graphene oxide, J. Mol. Liq., 209 (2015) 50–57.

[26] F. Najafi, O. Moradi, M. Rajabi, M. Asif, I. Tyagi, S. Agarwal, V.K. Gupta, Thermodynamics of the adsorption of nickel ions from aqueous phase using graphene oxide and glycine functionalized graphene oxide, J. Mol. Liq., 208 (2015) 106–113.

[27] J.P. Ruparelia, S.P. Duttagupta, A.K. Chatterjee, S. Mukherji, Potential of carbon nanomaterials for removal of heavy metals from water, Desalination, 232 (2008) 145–156.

[28] A. Aluigi, C. Tonetti, C. Vineis, C. Tonin, G. Mazzuchetti, Adsorption of copper(II) ions by keratin/PA6 blend nanofibres, Euro. Polym. J., 47 (2011) 1756–1764.

[29] H. Wang, P. Zhang, X. Ma, S. Jiang, Y. Huang, L. Zhai, S. Jiang, Preparation, characterization of electrospun meso-hydroxylapatite nanofibers and their sorptions on Co(II), J. Hazard. Mater., 265 (2014) 158–165.

[30] M. Aliabadi, M. Irani, J. Ismaeili, S. Najafzadeh, Design and evaluation of chitosan/hydroxyapatite composite nanofiber membrane for the removal of heavy metal ions from aqueous solution, J. Taiwan Inst. Chem. Eng., 45 (2014) 518–526.

[31] M.V. Dinu, E.S. Dragan, Evaluation of Cu^{2+}, Co^{2+} and Ni^{2+} ions removal from aqueous solution using a novel chitosan/clinoptilolite composite: kinetics and isotherms, Chem. Eng. J., 160 (2010) 157–163.

[32] G.P. Kumar, P.A. Kumar, S. Chakraborty, M. Ray, Uptake and desorption of copper ion using functionalized polymer coated silica gel in aqueous environment, Sep. Purif. Technol., 57 (2007) 47–56.

[33] D. Vu, Zh. Li, H. Zhang, W. Wang, Z. Wang, X. Xu, B. Dong, C. Wang, Adsorption of Cu(II) from aqueous solution by anatase mesoporous TiO_2 nanofibers prepared via electrospinning, Colloid Interface Sci., 367 (2012) 429–435.

[34] V.C. Srivastava, I.D. Mall, I.M. Mishra, Equilibrium modelling of single and binary adsorption of cadmium and nickel onto bagasse fly ash, Chem. Eng. J., 117 (2006) 79–91.

[35] S. Berber-Mendoza, R. Leyva-Ramos, J. Mendoza-Barron, R.M. Guerrero-Coronado, competitive exchange of lead(II) and cadmium(II) from aqueous solution on clinoptilolite, Stud. Surface Sci. Catal., 142 (2002)1849–1856.

[36] V.C. Srivastava, I.D. Mall, I.M. Mishra, Removal of cadmium(II) and zinc(II) metal ions from binary aqueous solution by rice husk ash, Colloids Surfaces A, 312 (2008) 172–184.

[37] C. Sheindorf, M. Rebhun, M. Sheintuch, A Freundlich-type multicomponent isotherm, J. Colloid Interface Sci., 79 (1981) 136–142.
[38] A.Z.M. Badruddoza, Z.B.Z. Shawon, T.W.J. Daniel, K. Hidajat, M.S. Uddin, Fe_3O_4/cyclodextrin polymer nanocomposites for selective heavy metals removal from industrial wastewater, Carbohydr. Polym., 91 (2013) 322–332.
[39] G.R. Mirzabe, A.R. Keshtkar, Application of response surface methodology for thorium adsorption on PVA/Fe_3O_4/SiO_2/APTES nanohybrid adsorbent, J. Ind. Eng. Chem., 26 (2015) 277–285.
[40] A. Sari, D. Mendil, M. Tuzen, M. Soylak, Biosorption of Cd(II) and Cr(III) from aqueoussolution by moss (*Hylocomium splendens*) biomass: equilibrium, kinetic and thermodynamic studies, Chem. Eng. J., 144 (2008) 1–9.
[41] A. Sari, M. Tuzen, Biosorption of cadmium(II) from aqueous solution by red algae (*Ceramium virgatum*): equilibrium, kinetic and thermodynamic studies, J. Hazard. Mater., 157 (2008) 448–454.
[42] Sumanjit, Seema, R.K. Mahajan, V.K. Gupta, Modification of surface behaviour of Eichhornia crassipes using surface active agent: an adsorption study, J. Ind. Eng. Chem., 21 (2015) 189–197.
[43] S. Kaur, S. Rani, R.K. Mahajan, M. Asif, V.K. Gupta, Synthesis and adsorption properties of mesoporous material for the removal of dye safranin: kinetics, equilibrium, and thermodynamics, J. Ind. Eng. Chem., 22 (2015) 19–27.
[44] Y. Liu, Y.J. Liu, Biosorption isotherms, kinetics and thermodynamics, Sep. Purif. Technol., 61 (2008) 229–242.
[45] C.C. Liu, M. Kuang-Wang, Y.S. Li, Removal of nickel from aqueous solution using wine processing waste sludge, Ind. Eng. Chem. Res., 44 (2005) 1438–1445.